Functional characterization of a GGPPS variant identified in atypical femoral fracture patients and delineation of the role of GGPPS in bone-relevant cell types

Neus Roca-Ayats[1§], MSc; Pei Ying Ng[2§], PhD; Natàlia Garcia-Giralt[3*], PhD; Maite Falcó-Mascaró[1], MSc; Mónica Cozar[1]; Josep Francesc Abril[4], PhD; José Manuel Quesada Gómez[5], MD, PhD; Daniel Prieto-Alhambra, MD PhD[6,7]; Xavier Nogués[3], MD, PhD; James E. Dunford[7], PhD; R Graham Russell[7,8], MD PhD; Roland Baron[2], DDS, PhD; Daniel Grinberg[1†], PhD; Susana Balcells[1†], PhD; Adolfo Díez-Pérez[3†], MD PhD.
[§]Co-first authors
[†]Co-last authors

[1]Department of Genetics, Microbiology and Statistics, Facultat de Biologia, Universitat de Barcelona, Centro de Investigación Biomédica en Red de Enfermedades Raras (CIBERER), ISCIII, IBUB, IRSJD, Barcelona, Catalonia, Spain.
[2]Division of Bone and Mineral Research, Department of Oral Medicine, Harvard School of Dental Medicine, and Department of Medicine, Harvard Medical School, Boston, MA, United States
[3]Musculoskeletal Research Group, IMIM (Hospital del Mar Medical Research Institute), Centro de Investigación Biomédica en Red en Fragilidad y Envejecimiento Saludable (CIBERFES), ISCIII, Barcelona, Catalonia, Spain.
[4]Department of Genetics, Microbiology and Statistics, Facultat de Biologia, Universitat de Barcelona, IBUB; Barcelona, Catalonia, Spain.
[5]Mineral Metabolism Unit, Instituto Maimónides de Investigación Biomédica de Córdoba (IMIBIC), Hospital Universitario Reina Sofía, CIBERFES, ISCII, Córdoba, Spain.
[6]GREMPAL (Grup de Recerca en Malalties Prevalents de l'Aparell Locomotor), Idiap Jordi Gol Primary Care Research Institute, CIBERFES, Autonomous University of Barcelona, Barcelona, Spain.
[7]NIHR Musculoskeletal BRU & Botnar Research Centre, Nuffield Department of Orthopaedics, Rheumatology and Musculoskeletal Sciences, University of Oxford, Oxford, United Kingdom.
[8]The Mellanby Centre for Bone Research, Department of Oncology and Metabolism, University of Sheffield, Sheffield, United Kingdom.

Corresponding author:
[*]Natalia Garcia-Giralt, PhD, IMIM-Hospital del Mar, C/ Dr. Aiguader 88, 08003 Barcelona, SPAIN
E-mail: ngarcia@imim.es
Phone: 0034933160497; FAX:0034933160410

Supplemental data have been included with the submission

Grant supporters

Funds for the study include grants SAF2014-56562R, SAF2016-75948-R (Spanish MINECO), PI12/02315 (FIS, ISCII), 2014SGR932 (Catalan Government), and CIBERER (U720). This work was also supported by the Centro de Investigación Biomédica en Red en Fragilidad y Envejecimiento Saludable (CIBERFES; CB16/10/00245) and FEDER funds. JED was supported by the NIHR Biomedical Research Centre, Oxford. NR is recipient of a FPU predoctoral fellowship from the Spanish Ministerio de Educación Cultura y Deporte. The work was also supported by a grant from the US government, NIH, NIAMS (R01 AR062054) to R.B.

Abstract

Atypical femoral fractures (AFFs) are a rare but potentially devastating event, often but not always linked to bisphosphonate (BP) therapy. The pathogenic mechanisms underlying AFFs remain obscure, and there are no tests available that might assist in identifying those at high risk of AFF. We previously used exome sequencing to explore the genetic background of three sisters with AFFs and three additional unrelated AFF cases, all previously treated with BPs. We detected 37 rare mutations (in 34 genes) shared by the three sisters. Notably we found a p.Asp188Tyr mutation in the enzyme geranylgeranyl pyrophosphate synthase, a component of the mevalonate pathway, which is critical to osteoclast function, and is inhibited by N-BPs. In addition, the *CYP1A1* gene, responsible for the hydroxylation of 17β-estradiol, estrone, and vitamin D, was also mutated in all three sisters and one unrelated patient. Here we present a detailed list of the variants found, and report functional analyses of the *GGPS1* p.Asp188Tyr mutation, which showed a severe reduction in enzyme activity together with oligomerization defects. Unlike BP treatment, this genetic mutation will affect all cells in the carriers. RNAi knock-down of *GGPS1* in osteoblasts produced a strong mineralisation reduction and a reduced expression of osteocalcin, osterix and RANKL, whereas in osteoclasts, it led to a lower resorption activity. Taken together, the impact of the mutated GGPPS and the relevance of the downstream effects in bone cells make it a strong candidate for AFF susceptibility. We speculate that other genes such as *CYP1A1* might be involved in AFF pathogenesis, which remains to be functionally proved. The identification of the genetic background for AFFs provides new insights for future development of novel risk assessment tools.

Keywords

Atypical femoral fractures, bisphosphonate**s,** *GGPS1,* WES

Introduction

Osteoporosis with its associated fractures is the most common post-menopausal bone disorder but it also affects older men and women of all ethnicities. Nitrogen-containing bisphosphonates (N-BPs), are currently the most commonly used treatments for osteoporotic disease in millions of patients worldwide. Although the clinically important anti-fracture efficacy of BPs and their overall safety have been robustly demonstrated in several clinical trials[1] and systematic reviews,[2, 3] a number of uncommon adverse effects potentially associated with prolonged use of these drugs have also been described, among them atypical femoral fractures (AFFs).[4] These fractures, characterized by their location in the subtrochanteric region or femoral shaft, are distinct from classic osteoporotic fragility fractures.[5]

The pathogenic mechanisms underlying AFFs remain obscure, and there has been much speculation about the causes.[5] Given the low absolute incidence of AFFs, it may be hypothesized that rare underlying genetic causes may increase susceptibility to these fractures, which may then occur spontaneously or be triggered after additional interactions with bisphosphonates (BPs) or other anti-resorptive drugs. Currently there are no tests available, genetic or biochemical, which may assist in identifying those at high risk of AFFs. Identification of genetic determinants of AFF would therefore shed light on aetiological mechanisms and lead not only to novel diagnostic and risk algorithms for the millions of patients taking bisphosphonates for either osteoporosis or cancer-related bone disease, but also to possible therapeutic strategies for patients with delayed fracture or non-union.

Previously, we identified three sisters who have been treated with BPs for over 5 years and diagnosed with AFFs.[6] This observation suggested that a patient's genetic background may predispose the individual to AFF following long-term BP therapy. Accordingly, we performed whole exome sequencing to identify potential AFF-related mutations in these three sisters and three other unrelated long-term BP-treated patients with AFFs. We identified several variants, which we list here. Among them, we identified the p.Asp188Tyr mutation in the geranylgeranyl diphosphate synthase (*GGPS1*) gene.[6] Given that this enzyme is a site of inhibition by bisphosphonates in the mevalonate pathway, we focused on the mutation found for further functional studies. We demonstrate that p.Asp188Tyr markedly reduced GGPP synthase activity. Using shRNA-mediated knockdown of *GGPS1* in both mouse calvarial and mouse macrophage cells lines, to recapitulate the global loss of synthase activity due to the p.Asp188Tyr mutation, we showed that loss of GGPPS function

resulted in defective osteoblast and osteoclast activity. Therefore, this mutation may possibly explain the bone fragility in these patients, possibly exacerbated by BP treatment.

MATERIALS AND METHODS

Subjects

For whole-exome sequencing analysis, six patients with AFFs who had received long-term (> 5 years) treatment with BPs were recruited: three sisters from Hospital Universitario Reina Sofía (Córdoba, Spain) and three unrelated women from Hospital del Mar (Barcelona, Spain). Given that the clinical phenotype may be related in the majority of cases to exposure to BPs, we also selected 3 women with more than 6 years of BP treatment but with no history of AFF. Baseline characteristics of AFF patients and controls are described in Supplemental Table S1. The three affected sisters, all with hypercholesterolemia, had been on statins and received regularly PPIs, but no glucocorticoids or other bone-acting agent except BPs. Their mother had a forearm fracture as well as two of the three sisters. Written informed consent was obtained from all patients in accordance with the regulations of the Clinical Research Ethics Committee of Parc de Salut Mar, which approved the study.

Whole-Exome Sequencing (WES)

DNA of patients with AFF was extracted from peripheral blood with the Wizard Genomic DNA Purification Kit (Promega, Madrid, Spain) and used for whole-exome sequencing in the CNAG platform (Barcelona, Spain) using an Agilent capture kit and Illumina sequencing (Supplemental Methodology). The bioinformatics analysis is detailed in Supplemental Methodology. Genetic variants were filtered according to the following premises: a) non-synonymous change, b) not previously described or with a Minor Allele Frequency < 0.005 in NCBI dbSNP Human Build 135 (http://www.ncbi.nlm.nih.gov/), 1000 genomes project and ExAC database, c) not present in NHLBI Go Exome Sequencing Project (ESP) (http://evs.gs.washington.eu/EVS/), and d) not present in in-house exomes of individuals drawn from the general population (n=8). Due to the small number of in-house exomes, variants were later searched for in the CSVS (Collaborative Spanish Variant Server), which at present includes data from 1644 Spanish individuals, most of them sequenced in the same facilities. SIFT,[7] PolyPhen,[8] Mutation Taster,[9] and conservation scores obtained from PhastCons[10] were used for prioritization sorting.

Genetic variant validation

Filtered mutations were validated by polymerase chain reaction (PCR) and automatic Sanger sequencing. Sequencing was performed bidirectionally using BigDye^{TM} v3.1 Terminator Cycle Sequencing Kit (Applied Biosystems), according to the manufacturer's instructions. Relevant validated mutations were *in silico* analyzed (Supplemental Methodology) and screened in 3 samples from women without atypical fracture and long-term bisphosphonate use, by Sanger sequencing.

GGPPS enzyme activity and conformation

The cDNA for both wild type and Asp188Tyr GGPPS were cloned into an inducible bacterial expression vector and the resulting His-tagged proteins were expressed overnight in transformed *E. coli* BL-21 (DE3) cells. Protein extracts were obtained and correct expression was verified by western blot using an anti-GGPPS antibody (sc-271680 Santa Cruz Biotechnology). GGPPS was purified from extracts using Ni sepharose followed by gel filtration chromatography. Analysis of the oligomerization of the GGPPS monomers was undertaken using a Sephadex S300 gel filtration column. Enzyme activity was assayed using substrates, Farnesyl pyrophosphate and C14-isopentenyl pyrophosphate (400KBq/μMol) at 20μM in buffer containing 100mM HEPES pH7.5, 2mM MgCl2, 0.1% Tween 20. Reactions were stopped after 10 mins at 37 ºC by the addition of acidified methanol. Reaction products were extracted directly into water immiscible scintillation fluid and quantified by scintillation counting.

Cell culture and transduction

MC3T3-E1 osteoblast/calvarial and RAW264.7 macrophage cell lines were cultured in complete α-MEM (10% fetal bovine serum, 100U/ml penicillin and 100U/ml streptomycin) and maintained in humidified conditions with 5% CO_2 at 37°C. To generate osteoblasts and macrophages depleted of *GGPS1* expression, MC3T3-E1 osteoblast/calvarial and RAW 264.7 macrophage cell lines were transduced with either five different GGPS1 MISSION shRNAs or non-target shRNA control lentiviral transduction particles (MilliporeSigma, St. Louis, MO, USA). Stable cell lines for MC3T3-E1 were established through puromycin selection at 2μg/ml. For RAW 264.7 macrophages, successfully transduced cells were selected using puromycin at 6μg/ml for 7-8 days. Once single cell-derived colonies were observed, three individual cell

colonies per shRNA were harvested using cell cloning cylinders and further expanded to form stable cell lines.

Mineralization assay and analysis

To assay for mineralization activity, stably transduced MC3T3-E1 cells were plated in 24-well plates and cultured in osteogenic media (complete α-MEM with 2μg/ml of puromycin, 50μg/ml L-ascorbic acid and 10mM β-glycerophosphate). Osteogenic media was replaced every three days and cells were fixed with 4% paraformaldehyde (PFA) after 21 days. Bone nodules were stained using Alizarin Red solution and bone nodule area (mm^2) were quantified using the Fiji software.

Osteoclast culture and resorption assay

Stably transduced RAW 264.7 macrophages were differentiated into osteoclasts in differentiation media (complete α-MEM with 6μg/ml of puromycin, supplemented with 10ng/ml recombinant mouse RANKL (R&D Systems, Minneapolis, MN, USA)). Media was changed every 48 hours and after four days, cells were fixed with 4% PFA. Cells positive for TRAP activity and containing three or more nuclei were scored as mature osteoclasts. To assess resorptive activity, macrophages were plated onto 24-well Osteo Assay Surface plates (Corning, Lowell, MA, USA) and cultured in differentiation media for seven days. Media was aspirated from the wells at the end of day 7 and cells were gently removed using a 10% bleach solution. The wells were washed with distilled water and dried well before a Von Kossa stain was performed to contrast between resorption pits formed and the surface coating. Six random fields per well were imaged using light microscopy and the percentage of resorbed area was analyzed using the Fiji software.

RESULTS

Variants detected in WES

The three sisters (AFS1, AFS2, AFS3) and the three unrelated patients (AFU1, AFU2, AFU3) were distributed into two groups and analyzed separately. The workflow and number of identified variants are shown in Fig. 1. In a first step, only mutations shared by the three sisters were taken into account both in a dominant and a recessive model. No variants were identified in homozygosis, whereas 74 variants were identified in heterozygosis (consistent with a dominant model), 37 of which were validated by Sanger sequencing. In

three genes (*FN1*, *BRAT1* and *XAB2*), the sisters were found to carry two different mutations. Direct visualization of sequence reads with the IGV software as well as polymorphism analyses indicated that the variants were in phase in all cases, being double-mutant alleles rather than compound heterozygotes. The 37 coding variants shared by the three sisters, all missense except for one nonsense and one in-frame deletion, are listed in Supplemental Table S2, according to their conservation score. The first variant in the list, with the best conservation score, was in the *GGPS1* gene, as we previously described.[6]

In a second step, the genes with variants shared by the sisters were screened in the WES results of the unrelated patients using the IGV software. None of the variants was found in any of the unrelated patients. However, in *BRAT1* and *CYP1A1*, two other variants were found in AFU3 and AFU1, respectively (Supplemental Table S3). The *CYP1A1* variant present in AFU1 (p.Ser216Cys) is a change of a serine to a sulphur-containing amino acid next to the substrate binding site and is predicted to be very deleterious to its function. Likewise, the *CYP1A1* variant present in the sisters (p.Arg98Trp) is a very significant change of a basic (arginine) to an aromatic hydrophobic amino acid (tryptophan), lying in a hydrogen-bonded turn of the protein. Conversely, the three variants detected in the *BRAT1* gene (two of them in the three sisters, in a double-mutant allele, and one in patient AFU3) were predicted as unlikely to affect its function. None of the variants in Supplemental Tables S2 and S3 was found in 3 controls (long-term treated with BPs but without AFFs). A total of 11 mutations are not present either in the NCBI dbSNP or in ExAC. The other variants, without MAF in dbSNP, have allele frequencies ≤ 2/10,000 according to ExAC. Only 10 variants are present in the CSVS database, all but one (in *FN1*) with allele frequencies < 5/1000, in the Iberian population (Supplemental Table S2).

Functional analyses of the GGPPS mutation

Asp188 is an active site residue of GGPP synthase, involved in the binding of the substrate via a magnesium salt bridge. Disruption of this residue is expected to lead to a vastly reduced rate of activity. To confirm this prediction, we produced mutant and wildtype recombinant GGPPS enzymes (Fig. 2*A*) and assayed their activity *in vitro*. As shown in Fig. 2*B*, the mutant displayed 5.7% of wild-type activity, with values of 0.72±0.09 cpm/ng/min for the wildtype and 0.04±0.013 cpm/ng/min for the mutant (n=3). Gel filtration experiments using a calibrated S300 column showed the wildtype enzyme as having a molecular weight in excess of 220 kDa, indicative of the expected hexameric conformation, in line with previous findings.[11] The mutant enzyme

consistently showed two peaks corresponding to the hexamer and to the monomer (peak at approximately 38 kDa), suggesting the mutation has a destabilizing effect on the oligomerization of the enzyme (Fig. 2*C*).

Next, we studied the effect of GGPPS depletion *in vitro* by utilizing shRNA mediated knockdown of *GGPS1* in MC3T3-E1 and RAW 264.7 cells. To this end, five independent shRNAs against *GGPS1* (denoted #1 to #5) and a control non-targeting shRNA were initially screened for their efficacy in depleting *GGPS1* mRNA expression in MC3T3-E1 cells. mRNA expression levels were examined using RT-qPCR. Of the five shRNAs, only shRNAs #1 and #2 exhibited promising potential knock-down effects at the mRNA level in MC3T3-E1 cells (>50%) (Fig. 3*A*). However, when subjected to immunoblot analysis, only shRNA #1 showed a strong reduction of *GGPS1* at the protein level (Fig. 3*B*). As such, only shRNA #1 was used in further experiments. Control and *GGPS1*-depleted MC3T3-E1 cells were cultured under mineralizing conditions and stained with alizarin red (Fig. 3*C*). Bone nodule formation *in vitro* was dramatically reduced following *GGPS1* inhibition (Fig. 3*D*). To assess whether the impaired mineralization activity of *GGPS1*-depleted MC3T3-E1 cells were a result of impaired osteoblast differentiation, we further analyzed the mRNA expression of key osteoblast markers using RT-qPCR. Interestingly, there were clear reductions in *RANKL*, *OSX* and *OCN* mRNA expression in *GGPS1*-depleted cells (Fig. 3*E*), while no significant effects were observed for *RUNX2*, *ALPL*, *MEPE* and *PHEX*.

Similarly, RAW 264.7 mouse macrophages were transduced with the same five shRNAs against *GGPS1* and a non-targeting shRNA control. Initial screening of the resultant five heterogenous polyclonal pool of stable RAW 264.7 cells using RT-qPCR indicated that *GGPS1* knockdown efficiency was lower than expected (data not shown). As such, 2-3 monoclonal stables for each *GGPS1*-shRNA were generated (denoted shRNA #1A-C, #2A-B, #3A-C, #4A-C, and #5A-B). Using RT-qPCR, we again screened for the efficiency of *GGPS1* knockdown and found that monoclonal stable cell lines generated from shRNAs #1C, #2B and #4B yielded the most potent effects, achieving consistent knockdown of *GGPS1* at the mRNA level (>65%) (Fig. 4*A*). At the protein level however, only macrophages generated from *GGPS1* shRNA #4A exhibited a significantly decreased protein expression of *GGPS1* (Fig. 4*B*), and was therefore selected for further analyses.

To assess whether *GGPS1* was functionally required during osteoclast formation, control and *GGPS1* knockdown cells were plated in 24-well plates in triplicates and treated with RANKL every 48 hours over a course of 4 days. Cells were fixed with 4% PFA, stained for TRAP, and imaged using light microscopy (Fig. 4*C*). When quantitated, we found that loss of *GGPS1* expression increased osteoclast formation significantly

(Fig. 4*D*). Lastly, to examine if *GGPS1* was necessary for resorptive activity, control and *GGPS1* knockdown cells were cultured on Osteo Assay Surface plates for a course of 7 days, supplemented with RANKL every 48 hours. Both TRAP activity and F-actin ring formation in *GGPS1* knockdown osteoclasts appeared indistinguishable from the control, and *GGPS1* knockdown osteoclasts also appeared to retain some resorptive abilities (Fig. 4*E*). However, when the resorptive pits were quantitated, we found that *GGPS1*-depleted osteoclasts had decreased resorption area although it did not reach significance (Fig. 4*F*).

DISCUSSION

In the present study, we describe the list of rare variants identified by WES in three sisters affected with AFF. Since causality cannot be attributed to rare variants that segregate within a small family just because they are rare,[12,13] we have carefully analyzed the function of the most interesting variant, the p.Asp188Tyr mutation in *GGPS1*, which we recently reported elsewhere.[6] The results presented here provide functional evidence of pathogenicity of this *GGPS1* mutation and its role in regulating bone cells and their activities.

The *GGPS1* gene encodes the GGPPS enzyme involved in the mevalonate pathway (Supplemental Fig. S1), and along with farnesyl pyrophosphate synthase (FPPS), is known to be inhibited by a variety of N-BPs.[14] The primary function of the mevalonate pathway is the production of cholesterol, as well as the synthesis of isoprenoid lipids, including farnesyl diphosphate (FPP) and geranylgeranyl diphosphate (GGPP),[15] which are required for the post-translational modification (prenylation) of some proteins. The geranylgeranyl diphosphate synthase enzyme (GGPPS) catalyzes the synthesis of geranylgeranyl diphosphate (GGPP) from farnesyl diphosphate and isopentenyl diphosphate. GGPPS functions as a homohexamer, in which each monomer binds 3 Mg^{2+} ions.[11]

We clearly show that the p.Asp188Tyr (D188Y) mutation severely impairs *in vitro* enzyme activity, consistent with the fact that it lies in the second aspartate rich region, highly conserved across all GGPPS and FPPS, and involved in the binding of the substrates to the enzyme active site *via* a Mg^{2+} salt bridge, which is essential for catalytic activity. It is well known that any disruption in this region results in an almost complete loss of activity.[16] We also show, by gel filtration experiments, that the p.D188Y mutation destabilizes the homohexameric conformation of the enzyme elucidated by Kavanagh *et al*.[11] Taken all the data together, and according to the American College of Medical Genetics and Genomics criteria,[17] this mutation is classified as pathogenic, even though it has not been reported in any additional AFF patient, so far.

To examine the functional role of GGPPS in bone cells, we performed *in vitro* studies in *GGPS1*-depleted osteoblasts or osteoclasts. GGPPS-depleted MC3T3 cells had reduced mineralization capacity and reduced gene expression of osteocalcin, osterix and RANKL. These results are in agreement with those of Weivoda & Hohl,[18] in which GGPPS was inhibited with digeranyl bisphosphonate (DGBP) in MC3T3 cells. These authors suggested that the observed lack of mineralization and the decrease in *ALPL* and *OCN* gene expression were due to the accumulation of FPP, and its subsequent activation of the glucocorticoid receptor,[19] which is known to inhibit osteoblast proliferation and bone formation, and to increase osteoblast apoptosis.[20] In addition, the depletion of RANKL would lead to an aberrant osteoblast-osteoclast cross-talk. The effect of GGPPS depletion in osteoclasts was an increase in cell number and a slightly decreased activity. Disruption of *GGPS1* as depicted in our shRNA assay, is predicted to reduce the synthesis of GGPP. Depletion of GGPP impairs the prenylation of GTPases such as Rho, Rac, Rap1 and Rabs, which have been shown to play essential roles in both osteoclast formation and function.[21-25] Mouse models utilizing osteoclast targeted depletion or global depletion of these key GTPases have shown conflicting trends in the resulting osteoclast numbers, which is not well understood, and might stem from the different ages at which the different laboratory groups analyzed their mice specimen.[23, 25] Interestingly, however, all of the mice models exhibited osteopetrotic phenotypes, indicating that osteoclast resorptive activity is highly dependent on geranylgeranylation.[23-26] Unlike these previous studies, our work in disrupting *GGPS1* does not specifically target any of the GTPases mentioned. Loss of prenylation and membrane localization of these GTPases following GGPPS depletion does not necessarily translate to inhibited GTPase function. In fact, it has been shown that unprenylated GTPases can remain in the GTP-bound form, accumulate in the cytosol and retain partial functional activity such as inducing activation of the p38 MAPK,[27] which is an important signaling pathway for osteoclast differentiation and formation.[28] Therefore, despite the increased osteoclast numbers in our *GGPS1* shRNA population, there is a slight decrease in bone resorptive activity, consistent with previous studies showing that geranylgeranylation plays a pivotal role during osteoclast bone resorption due to alterations in vesicular traffic, a cellular function possibly less essential during osteoclast differentiation.

Of note, and unlike BPs which preferentially target osteoclasts, the GGPPS mutation in the three sisters will affect all of their cells, including osteoblasts. Because the administration of bisphosphonate targets mainly

FPP synthase, which is upstream of GGPPS, we speculate that the effect of bisphosphonates on the cell lines will be compounded due to the loss of both farnesylation and geranylgeranylation. However, while the relevant cell lines may reveal some answers, they may not fully replicate what happens in clinical cases, where *in vivo* osteoblast and osteoclast responses are intimately associated due to their coupling in bone remodeling. Furthermore, it appears that the onset of atypical femoral fractures usually occurs following prolonged bisphosphonate treatment, which is difficult to mimic in an *in vitro* environment. Developing an animal model strategy should provide more compelling evidence. The *GGPS1*-BP interaction is also supported by the finding of a common variant in the *GGPS1* promoter which was associated with lack of BMD improvement after BP therapy,[29] possibly indicating that the pathway was already impaired in these patients.

Another interesting potentially causative gene in our list is *CYP1A1*, which was found mutated in the three sisters, in one of our unrelated AFF patients, and also in another AFF patient reported elsewhere.[30] According to the American College of Medical Genetics and Genomics criteria,[17] these *CYP1A1* mutations may be classified as likely pathogenic. Functional studies needed to confirm their pathogenicity are underway. *CYP1A1* encodes a member of the cytochrome P450 superfamily, involved in the metabolism of drugs and xenobiotics and arises as a good AFF-susceptibility candidate since it is responsible for the hydroxylation of 17β-estradiol, estrone, and vitamin D in extrahepatic tissues.[31] Its role in bone biology is also supported by the association found between the *CYP1A1* C4887A polymorphism and a higher degree of estrogen catabolism and lower femoral BMD in postmenopausal women.[32]

The strengths of our study were the possibility to analyze three sisters with AFF and the choice of a hypothesis-free WES approach that allowed us to detect new variants not included in exon arrays, as previously performed.[33] On the other hand, the small number of AFF patients and controls studied here is an important limitation, and further WES of additional AFF cases are underway. Moreover, we could only analyze three sisters, who have an *a priori* chance of 1/8 of sharing any variant, which is above a conventional level of statistical significance.

In summary, our results show the negative impact of the GGPPS p.Asp188Tyr mutation and the relevance of the downstream effects in bone cells, which makes it a candidate for AFF susceptibility. In addition, our data show other potential AFF contributory genes, although functional studies are needed to prove their involvement in the pathology. Further identification and/or replication of genetic variants will be necessary to

detect at risk individuals and to decide which patients are suitable for being treated with BPs with no risk of this side effect.

Disclosures

All authors state that they have no conflicts of interest.

Acknowledgements

We thank the patients for their kind participation. Funds for the study include grants SAF2014-56562R, SAF2016-75948-R (Spanish MINECO), PI12/02315 (FIS, ISCII), 2014SGR932 (Catalan Government), and CIBERER (U720). This work was also supported by the Centro de Investigación Biomédica en Red en Fragilidad y Envejecimiento Saludable (CIBERFES; CB16/10/00245) and FEDER funds. JED was supported by the NIHR Biomedical Research Centre, Oxford. NR is recipient of a FPU predoctoral fellowship from the Spanish Ministerio de Educación Cultura y Deporte. The work was also supported by a grant from the US government, NIH, NIAMS (R01 AR062054) to RB.

Authors' roles: Study design: ADP, NGG, SB, and DG. Study conduct: NRA, PYN, NGG, MFM, MC, JFA, and JED. Patient and data collection: JMQG, XN, and DPA. Data analysis: NRA, PYN, NGG, MFM, JFA, GGR, RB, DG, SB, ADP. Data interpretation: All authors. Drafting manuscript: NRA, PYN, NGG, JED, GGR, RB, DG, SB, ADP. Revising manuscript content: All authors. Approving final version of manuscript: All authors. NRA and PYN take responsibility for the integrity of the data analysis.

References

1. Freemantle N, Cooper C, Diez-Perez A, Gitlin M, Radcliffe H, Shepherd S, et al. Results of indirect and mixed treatment comparison of fracture efficacy for osteoporosis treatments: a meta-analysis. Osteoporos Int. 2013;24(1):209-17.

2. Zhou J, Ma X, Wang T, Zhai S. Comparative efficacy of bisphosphonates in short-term fracture prevention for primary osteoporosis: a systematic review with network meta-analyses. Osteoporos Int. 2016;27(11):3289-300.

3. Peng J, Liu Y, Chen L, Peng K, Xu Z, Zhang D, et al. Bisphosphonates can prevent recurrent hip fracture and reduce the mortality in osteoporotic patient with hip fracture: A meta-analysis. Pak J Med Sci. 2016;32(2):499-504.

4. Kennel KA, Drake MT. Adverse effects of bisphosphonates: implications for osteoporosis management. Mayo Clin Proc. 2009;84(7):632-7; quiz 8.

5. Shane E, Burr D, Abrahamsen B, Adler RA, Brown TD, Cheung AM, et al. Atypical subtrochanteric and diaphyseal femoral fractures: second report of a task force of the American Society for Bone and Mineral Research. J Bone Miner Res. 2014;29(1):1-23.

6. Roca-Ayats N, Balcells S, Garcia-Giralt N, Falco-Mascaro M, Martinez-Gil N, Abril JF, et al. GGPS1 Mutation and Atypical Femoral Fractures with Bisphosphonates. N Engl J Med. 2017;376(18):1794-5.

7. Kumar P, Henikoff S, Ng PC. Predicting the effects of coding non-synonymous variants on protein function using the SIFT algorithm. Nat Protoc. 2009;4(7):1073-81.

8. Adzhubei IA, Schmidt S, Peshkin L, Ramensky VE, Gerasimova A, Bork P, et al. A method and server for predicting damaging missense mutations. Nat Methods. 2010;7(4):248-9.

9. Schwarz JM, Cooper DN, Schuelke M, Seelow D. MutationTaster2: mutation prediction for the deep-sequencing age. Nat Methods. 2014 Apr;11(4):361-2.

10. Siepel A, Bejerano G, Pedersen JS, Hinrichs AS, Hou M, Rosenbloom K, et al. Evolutionarily conserved elements in vertebrate, insect, worm, and yeast genomes. Genome Res. 2005;15(8):1034-50.

11. Kavanagh KL, Dunford JE, Bunkoczi G, Russell RG, Oppermann U. The crystal structure of human geranylgeranyl pyrophosphate synthase reveals a novel hexameric arrangement and inhibitory product binding. J Biol Chem. 2006;281(31):22004-12.

12. MacArthur DG, Manolio TA, Dimmock DP, Rehm HL, Shendure J, Abecasis GR, et al. Guidelines for investigating causality of sequence variants in human disease . Nature. 2014;508(7497):469-76

13. Minikel EV, Vallabh SM, Lek M, Estrada K, Samocha KE, Sathirapongsasuti JF, et al. Quantifying prion disease penetrance using large population control cohorts. Sci Transl Med. 2016;8(322):322ra9.

14. Guo RT, Cao R, Liang PH, Ko TP, Chang TH, Hudock MP*, et al.* Bisphosphonates target multiple sites in both cis- and trans-prenyltransferases. Proc Natl Acad Sci U S A. 2007;104(24):10022-10027.

15. Goldstein JL, Brown MS. Regulation of the mevalonate pathway. Nature. 1990;343(6257):425-430.

16. Kavanagh KL, Guo K, Dunford JE, Wu X, Knapp S, Ebetino FH, et al. The molecular mechanism of nitrogen-containing bisphosphonates as antiosteoporosis drugs. Proc Natl Acad Sci U S A. 2006;103(20):7829-34.

17. Richards S, Aziz N, Bale S, Bick D, Das S, Gastier-Foster J, et al. Standards and guidelines for the interpretation of sequence variants: a joint consensus recommendation of the American College of Medical Genetics and Genomics and the Association for Molecular Pathology. Genet Med. 2015; 17(5):405-24.

18. Weivoda MM, Hohl RJ. The effects of direct inhibition of geranylgeranyl pyrophosphate synthase on osteoblast differentiation. J Cell Biochem. 2011;112(6):1506-13.

19. Das S, Schapira M, Tomic-Canic M, Goyanka R, Cardozo T, Samuels HH. Farnesyl pyrophosphate is a novel transcriptional activator for a subset of nuclear hormone receptors. Mol Endocrinol. 2007;21(11):2672-86.

20. Weinstein RS, Jilka RL, Parfitt AM, Manolagas SC. Inhibition of osteoblastogenesis and promotion of apoptosis of osteoblasts and osteocytes by glucocorticoids. Potential mechanisms of their deleterious effects on bone. J Clin Invest. 1998;102(2):274-82.

21. Zou W, Izawa T, Zhu T, Chappel J, Otero K, Monkley SJ, et al. Talin1 and Rap1 are critical for osteoclast function. Mol Cell Biol. 2013;33(4):830-44.

22. Pavlos NJ, Xu J, Riedel D, Yeoh JS, Teitelbaum SL, Papadimitriou JM, et al. Rab3D regulates a novel vesicular trafficking pathway that is required for osteoclastic bone resorption. Mol Cell Biol. 2005;25(12):5253-69.

23. Croke M, Ross FP, Korhonen M, Williams DA, Zou W, Teitelbaum SL. Rac deletion in osteoclasts causes severe osteopetrosis. J Cell Sci. 2011;124(Pt 22):3811-21.

24. Ito Y, Teitelbaum SL, Zou W, Zheng Y, Johnson JF, Chappel J, et al. Cdc42 regulates bone modeling and remodeling in mice by modulating RANKL/M-CSF signaling and osteoclast polarization. J Clin Invest. 2010;120(6):1981-93.

25. Itokowa T, Zhu ML, Troiano N, Bian J, Kawano T, Insogna K. Osteoclasts lacking Rac2 have defective chemotaxis and resorptive activity. Calcif Tissue Int. 2011;88(1):75-86.

26. Magalhaes JK, Grynpas MD, Willett TL, Glogauer M. Deleting Rac1 improves vertebral bone quality and resistance to fracture in a murine ovariectomy model. Osteoporos Int. 2011;22(5):1481-92.

27. Dunford JE, Rogers MJ, Ebetino FH, Phipps RJ, Coxon FP. Inhibition of protein prenylation by bisphosphonates causes sustained activation of Rac, Cdc42, and Rho GTPases. J Bone Miner Res. 2006;21(5):684-94.

28. Li X, Udagawa N, Itoh K, Suda K, Murase Y, Nishihara T, et al. p38 MAPK-mediated signals are required for inducing osteoclast differentiation but not for osteoclast function. Endocrinology. 2002;143(8):3105-13.

29. Choi HJ, Choi JY, Cho SW, Kang D, Han KO, Kim SW, et al. Genetic polymorphism of geranylgeranyl diphosphate synthase (GGSP1) predicts bone density response to bisphosphonate therapy in Korean women. Yonsei Med J. 2010;51(2):231-8.

30. Peris P, González-Roca E, Rodríguez-García SC, López-Cobo MM, Monegal A, Guañabens N. Incidence of Mutations in the ALPL, GGPS1, and CYP1A1 Genes in Patients With Atypical Femoral Fractures. JBMRPlus. 2018.

31. Zhou SF, Liu JP, Chowbay B. Polymorphism of human cytochrome P450 enzymes and its clinical impact. Drug Metab Rev. 2009;41(2):89-295.

32. Napoli N, Villareal DT, Mumm S, Halstead L, Sheikh S, Cagaanan M, et al. Effect of CYP1A1 gene polymorphisms on estrogen metabolism and bone density. J Bone Miner Res. 2005;20(2):232-9.

33. Perez-Nunez I, Perez-Castrillon JL, Zarrabeitia MT, Garcia-Ibarbia C, Martinez-Calvo L, Olmos JM, et al. Exon array analysis reveals genetic heterogeneity in atypical femoral fractures. A pilot study. Mol Cell Biochem. 2015;409(1-2):45-50.

Figure legends

Fig. 1. Flow chart of approach for detecting AFF-associated mutations.

Fig. 2. (*A*) Heterologous expression of WT and p.Asp188Tyr GGPPS, assessed by western blot of 2.5 μg of transformed non induced or IPTG-induced *E.coli* extracts (*B*) GGPPS enzyme activity in WT and p.Asp188Tyr mutant. p.Asp188Tyr GGPPS had a 5.7% of the WT activity, measured by scintillation counting

of [^{14}C]Geranylgeranyl pyrophosphate. Results are expressed as mean ± SD (n=3). ***p<0.001. (*C*) Gel filtration chromatograms for the WT GGPPS and the p.Asp188Tyr mutant. The WT enzyme appears to have a molecular weight of around 220 kDa, suggesting that it is present as a hexamer. The p.Asp188Tyr mutant enzyme consistently showed two peaks corresponding to the hexamer and the monomer (a peak around 38 kDa), suggesting that the mutant destabilizes the oligomerization of the enzyme.

Fig. 3. Effects of shRNA-mediated *GGPS1* depletion in MC3T3 cells. (*A*) qPCR analysis of shRNA-mediated knockdown of *GGPS1* expression. Data (mean ± SD) are shown as percent of mRNA levels in the negative control sample. (*B*) GGPPS protein expression levels measured by Western Blot. Data (means ± SD) are shown as relative protein levels with respect to the non-targeting sample. (*C*) Alizarin red staining of MC3T3 cells treated with the control shRNA or *GGPS1*-shRNA. (*D*) Quantification (%) of the area of mineralized nodule generated by MC3T3 cells treated with non-targeting shRNA or *GGPS1*- targeting shRNA. Results are expressed as mean ± SD. **p<0.01. (*E*) mRNA fold expression of osteoblast markers measured by RT-qPCR of control and *GGPS1*-shRNA-treated differentiated MC3T3 osteoblasts. Data (means ± SD) are shown as relative mRNA fold expression with respect to the non-targeting sample.

Fig. 4. Effects of shRNA-mediated *GGPS1* depletion in RAW264.7 macrophages after RANKL stimulation. (*A*) qPCR analysis of shRNA-mediated knockdown of *GGPS1* expression. Data (mean ± SD) are shown as percent of mRNA levels in the negative control sample. **p-value<0.01; ***p-value<0.001. (*B*) GGPPS protein expression levels in the selected samples measured by Western Blot. Data (means ± SD) are shown as relative protein levels with respect to the non-targeting sample. *p-value<0.05; **p-value<0.01. (*C*) Tartrate-resistant acid phosphatase (TRAP) staining of cells treated with the control shRNA or *GGPS1*-shRNA. (*D*) Quantification of osteoclasts derived from RAW264.7 cells treated with non-targeting shRNA or *GGPS1*-targeting shRNA. Results are expressed as mean ± SD. ***p<0.001. (*E*) TRAP staining, F-actin staining and resorptive pits generated after culturing cells on OsteoAssay surface plates of control and *GGPS1*-shRNA-treated cells. (*F*) Quantification (%) of the area of pits resorbed by control and *GGPS1*-shRNA-treated osteoclasts. Data are means ± SD.

Supplementary Figure S1. GGPPS participate in the mevalonate pathway: bisphosphonates act by inhibiting the FPPS, thereby preventing prenylation and activation of small GTPases that are essential for the activity and survival of osteoclasts.

Supplementary Table 2. Variants shared by the three sisters, found by exome sequencing

Gene	Protein	Variant[1]	Effect on the protein	dbSNP[2]	ExAC[3]	CSVS[4]	Mutation Taster[5]	Conservation[6]	Sift[7]	PolyPhen[8]
GGPS1	Geranylgeranyl diphosphate synthase	chr1:g.235505746G>T	p.D188Y				DC; 0.9999	700	**0.000**	**1.000**
LRRC1	Leucine-rich repeat-containing 1	chr6:g.53707020G>A	p.R91Q		4.946e-05	0.0003	DC; 0.9999	685	**0.050**	0.746
TUSC2	Tumor suppressor candidate 2	chr3:g.50363807T>C	p.H83R		8.244e-06		DC; 0.8891	674	0.338	0.000
SYDE2	Synapse defective 1, Rho GTPase, homolog 2	chr1:g.85634903G>T	p.L893I		8.339e-06	0.0003	DC; 0.9999	639	**0.018**	**0.997**
COG4	Component of oligomeric golgi complex 4	chr16:g.70553552C>T	p.G85D				DC; 0.9999	627	0.150	0.735
EML1	Echinoderm microtubule associated protein like 1	chr14:g.100360993G>A	p.R211H		6.611e-05		DC; 0.9999	588	**0.030**	**0.963**
KDM4C	Lysine(K)-specific demethylase 4C	chr9:g.6849579A>G	p.I170V	rs192832191 MAF=0.0004	2.471e-05		DC; 0.9999	584	**0.000**	0.509
ERCC6L2	Excision repair cross-complementation group 6 like 2	chr9:g.98718284A>T	p.I657L		8.278e-06		P; 0.9976	573	0.630	0.007
PGRMC1	Progesterone receptor membrane component 1	chrX:g.118377159C>A	p.P177H				DC; 0.9999	573	0.130	0.742
FN1*	Fibronectin 1	chr2:g.216235149C>T	p.V2241I		8.245e-06	0.0003	DC; 0.9997	551	**0.009**	0.045
CYP1A1	Cytochrome 450, family 1, subfamily A, polypeptide 1	chr15:g.75015147G>A	p.R98W		0.000108	0.0003	DC; 0.5242	540	**0.000**	**0.998**
XAB2*	XPA binding protein 2	chr19:g.7688142C>G	p.V385L		1.651e-05		DC; 0.9999	535	**0.007**	0.600
GPR20	G protein-coupled receptor 20	chr8:g.142367729C>T	p.D99N	rs200892677 MAF=0.0004	3.324e-05		DC; 0.9999	515	**0.000**	**0.998**
TMEM25	Transmembrane protein 25	chr11:g.118404174_ 118404176del	p.V239del				DC; 0.9999	510	N/A	N/A
NGEF	Guanine nucleotide exchange factor	chr2:g.233748153G>A	p.S542L		1.279e-05		DC; 0.9999	500	0.350	**0.910**
NKAP	NFκB activating protein	chrX:g.119066123C>T	p.S265N	rs182030723 MAF=0.0006	6.847e-05	0.0003	DC; 0.9999	497	0.120	0.184
NVL	Nuclear-VCP like	chr1:g.224491450G>A	p.T312I		8.268e-06		DC; 0.9999	474	**0.000**	**0.995**
FN1*	Fibronectin 1	chr2:g.216251538G>A	p.R1496W	rs139078629 MAF=0.003	0.004904	0.0103	DC; 0.9999	466	**0.005**	**0.998**
ATP6AP1	ATPase, H^+ transporting, lysosomal accessory protein 1	chrX:g.153664043G>A	p.V407I		4.561e-05		DC; 0.9868	464	0.260	**0.990**
LURAP1L	Leucine rich adaptor protein 1-like	chr9:g.12821722G>A	p.R217H		4.948e-05		P; 0.9289	452	0.270	0.371
HEPHL1	Hephaestin-like 1	chr11:g. 93839224G>A	p.W991*				DC; 1	451	**0.000**	N/A
NTPCR	Nucleoside-triphosphatase, cancer-related	chr1:g.233091444G>A	p.R59Q		5.779e-05		DC; 0.9997	439	**0.034**	0.502
XAB2*	XPA binding protein 2	chr19:g.7688159G>C	p.T379R		1.652e-05		DC; 0.9999	420	0.059	0.200
CHERP	Calcium homeostasis endoplasmic reticulum protein	chr19:g.16631044C>T	p.R793H	rs202164310 MAF=0.0000	0.0001009		DC; 0.9371	366	0.12	0.716
MEX3D	Mex-3 homolog D	chr19:g.1555839G>C	p.T560R	rs538022731 MAF=0.0002			P; 0.8576	336	**0.030**	N/A
BRAT1*	BRCA1-associated ATM activator	chr7:g.2594007C>T	p.R20K	rs143390199 MAF= 0.00002	1.651e-05		DC; 0.9349	333	0.192	0.010
BRAT1*	BRCA1-associated ATM activator	chr7:g.2580668G>A	p.T447M	rs368808380 MAF=0.0002	5.845e-05		P; 0.9999	333	0.110	0.275
CUL9	Cullin 9	chr6:g.43154714C>T	p.T423I				DC; 0.9979	251	**0.000**	**0.993**
ALPK1	Alpha-kinase 1	chr4:g.113353195A>C	p.D831A		0.0001255	0.0006	P; 0.9999	0	0.060	0.243

CD37	CD37 molecule	chr19:g.49840212C>G	p.I63M		2.476e-05	0.0003	P; 0.9999	0	**0.040**	0.028
IQCF6	IQ motif containing F6	chr3:g.51812782G>A	p.R61W				P; 0.9999	0	**0.010**	N/A
LFNG	LFNG O-fucosylpeptide 3-beta-N-acetylglucosaminyl-transferase	chr7:g.2566829C>T	p.R375C		1.69e-05		P; 0.9999	0	**0.020**	0.772
MGA	MAX dimerization protein	chr15:g.41988923C>T	p.S572L				P; 0.9999	0	0.130	N/A
POLI	Polymerase (DNA directed) iota	chr18:g.51820404T>C	p.V597A	rs543509008 MAF=0.0002	0.00024	0.0006	P; 0.9999	0	0.590	N/A
SHC4	SHC (Src homology 2 domain containing) family, member 4	chr15:g.49254675G>T	p.H180N			0.0003	P; 0.9999	0	1.000	0.000
SMS	Spermine synthase	chrX:g.21958982G>C	p.G14R				P; 0.9998	0	0.350	0.002
SNAPC4	Small nuclear RNA activating complex, polypeptide 4	chr9:g.139272279C>G	p.G1334R		2.675e-05	0.0006	P; 0.9999	0	0.160	0.707

[1]Genomic position of the variant in the human reference genome GRCh37
[2]Reference SNP ID number (rs) and MAF (minor allele frequency) for the already described variants
[3]Allele frequency for the already described variants in ExAC database
[4]Allele frequency for the already described variants in Collaborative Spanish Variant Server (CSVS) database (http://csvs.babelomics.org/)
[5]Prediction of disease potential by Mutation Taster and probability of the prediction. DC=Disease Causing; P=Polymorphism (http://www.mutationtaster.org/)
[6]Conservation score from PhastCons (0 to 1000), being 1000 the most conserved locus and 0 a non-conserved locus
[7]Sift: 0-0.05 damaging (in bold); 0.051-1 tolerable (non-damaging)
[8]PolyPhen: 0-0.4 benign; 0.41-0.89 possibly damaging; 0.9-1 pathogenic (in bold)
*Present in a double-mutant allele

Supplementary Table 3. Variants found in unrelated AFF patients in genes from Supplementary Table 2

Gene	Protein	Variant[1]	Effect on the protein	dbSNP[2]	ExAC[3]	CSVS[4]	Mutation Taster[5]	Conservation[6]	Sift[7]	PolyPhen[8]	AFF Patient
BRAT1	BRCA1-associated ATM activator	chr7:g.2580636C>T	p.E458K				P; 0.9999	333	0.568	0.000	AFU3
CYP1A1	Cytochrome 450, family 1, subfamily A, polypeptide 1	chr15:g.75014793T>A	p.S216C	rs146622566 MAF=0.0003	0.0001153		P; 0.9999	0	**0.004**	**0.987**	AFU1

[1]Genomic position of the variant in the human reference genome GRCh37
[2]Reference SNP ID number (rs) and MAF (minor allele frequency) for the already described variants
[3]Allele frequency for the already described variants in ExAC database
[4]Allele frequency for the already described variants in Collaborative Spanish Variant Server (CSVS) database (http://csvs.babelomics.org/)
[5]Prediction of disease potential by Mutation Taster and probability of the prediction. DC=Disease Causing; P=Polymorphism (http://www.mutationtaster.org/)
[6]Conservation score from PhastCons (0 to 1000), being 1000 the most conserved locus and 0 a non-conserved locus
[7]Sift: 0-0.05 damaging (in bold); 0.051-1 tolerable (non-damaging)
[8]PolyPhen: 0-0.4 benign; 0.41-0.89 possibly damaging; 0.9-1 pathogenic (in bold)

FIGURE 1

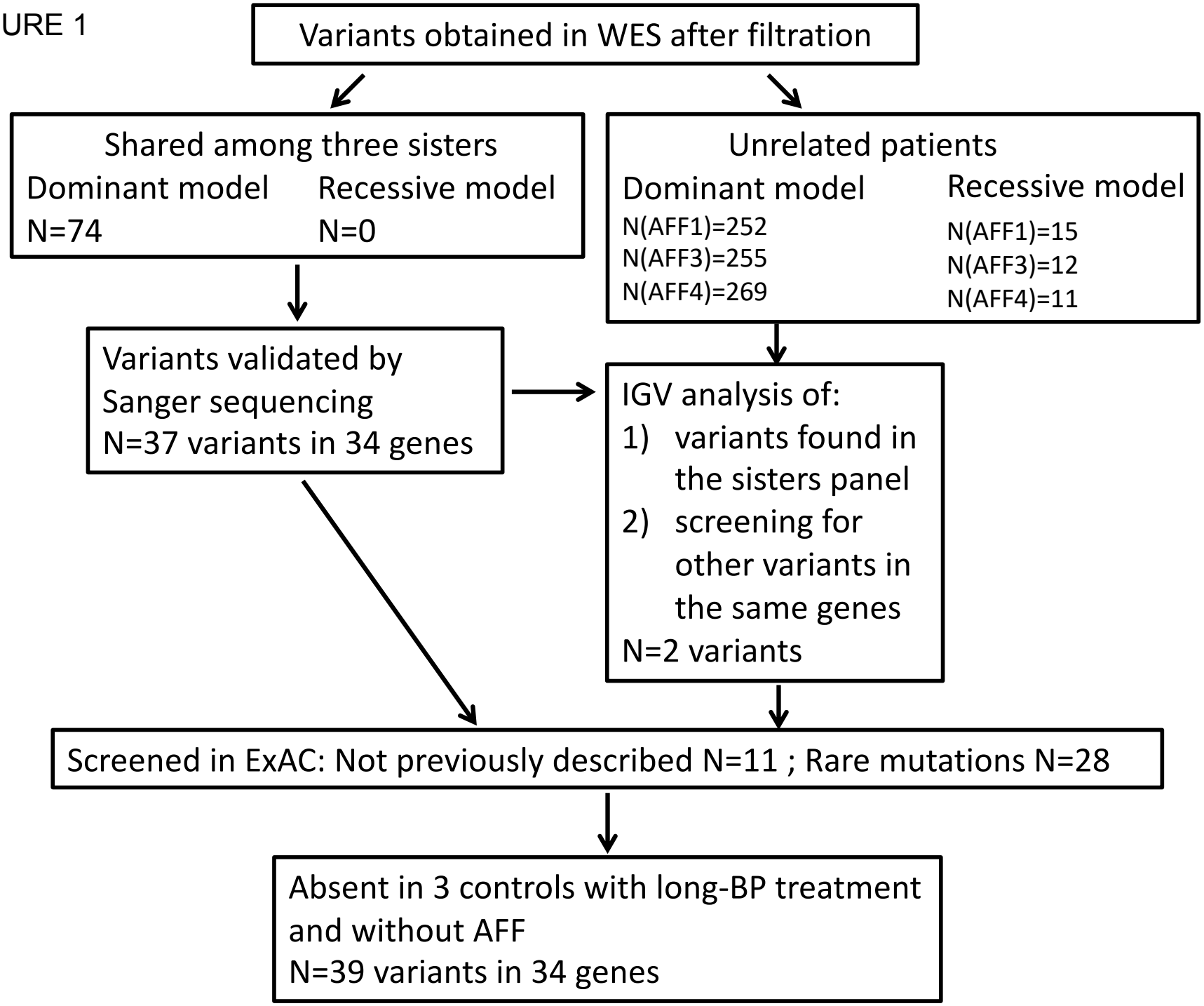
Variants obtained in WES after filtration
Shared among three sisters
Dominant model
N=74
Recessive model
N=0
Unrelated patients
Dominant model
N(AFF1)=252
N(AFF3)=255
N(AFF4)=269
Recessive model
N(AFF1)=15
N(AFF3)=12
N(AFF4)=11
Variants validated by Sanger sequencing
N=37 variants in 34 genes
IGV analysis of:
1) variants found in the sisters panel
2) screening for other variants in the same genes
N=2 variants
Screened in ExAC: Not previously described N=11 ; Rare mutations N=28
Absent in 3 controls with long-BP treatment and without AFF
N=39 variants in 34 genes

FIGURE 2

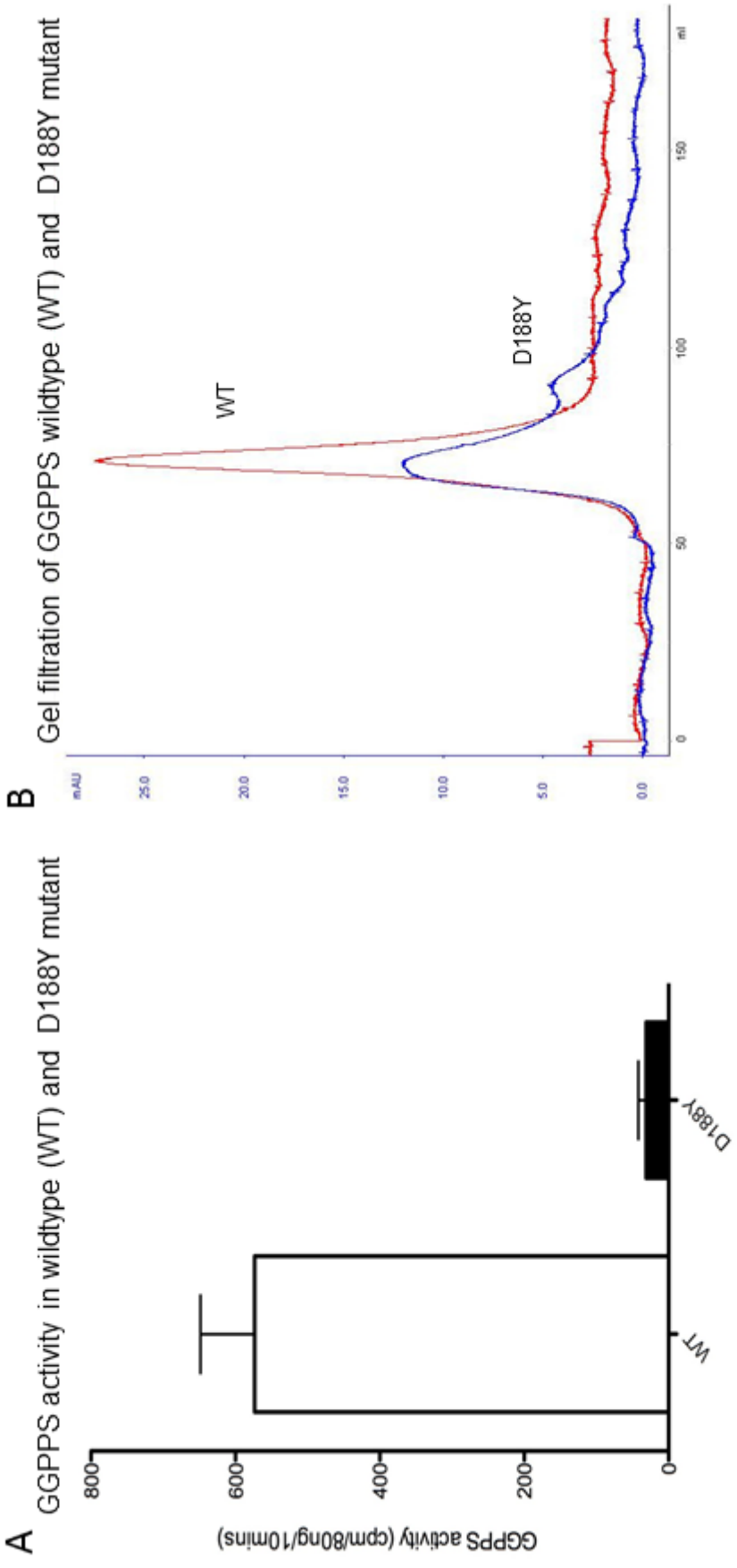
A
GGPPS activity in wildtype (WT) and D188Y mutant
GGPPS activity (cpm/80ng/10mins)
800
600
400
200
0
WT
D188Y
B
Gel filtration of GGPPS wildtype (WT) and D188Y mutant
mAU
25.0
20.0
15.0
10.0
5.0
0.0
WT
D188Y
0
50
100
150
ml

FIGURE 3

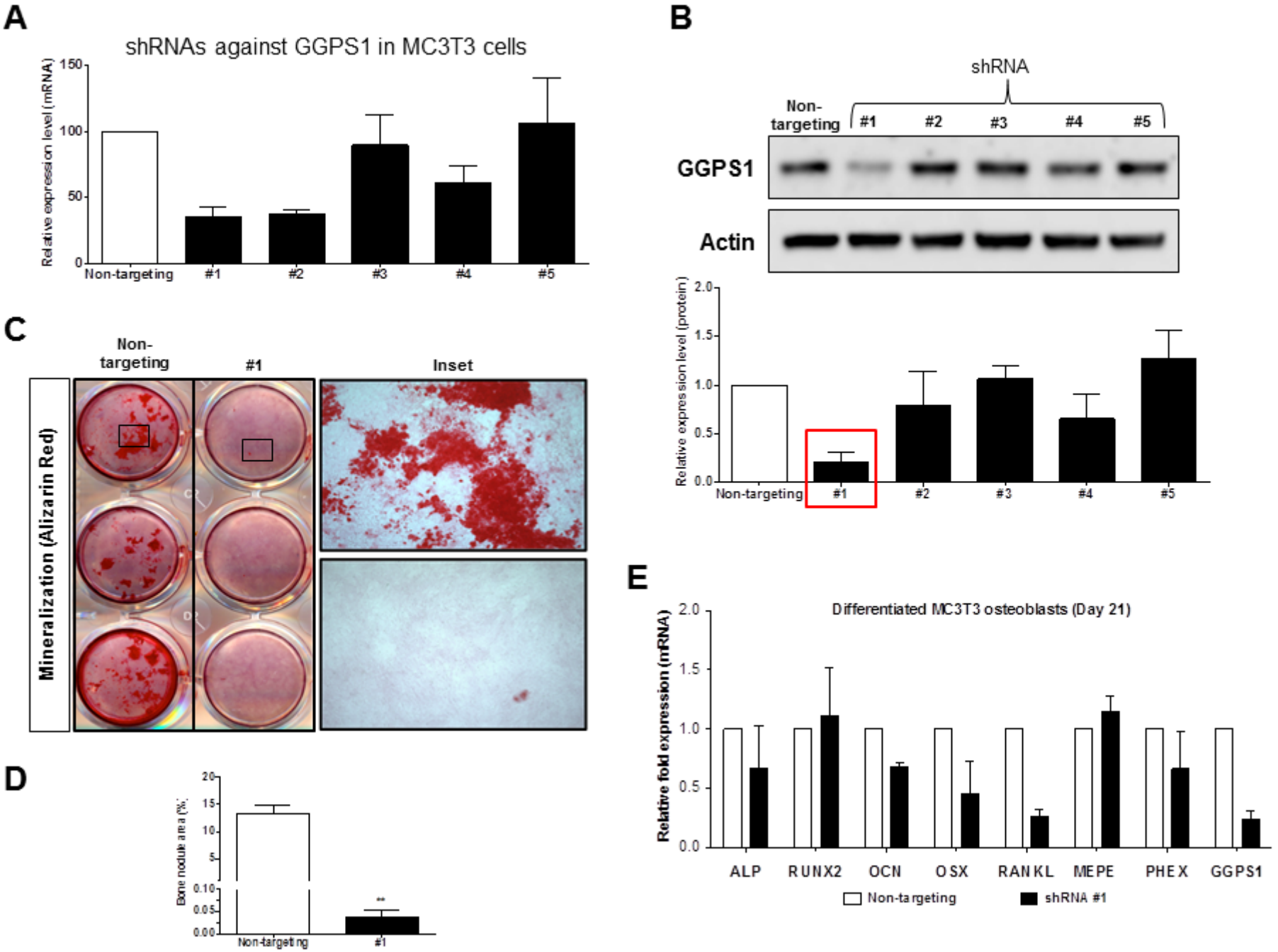
A
shRNAs against GGPS1 in MC3T3 cells
Relative expression level (mRNA)
150
100
50
0
Non-targeting
#1
#2
#3
#4
#5
B
shRNA
Non-targeting
#1
#2
#3
#4
#5
GGPS1
Actin
Relative expression level (protein)
2.0
1.5
1.0
0.5
0.0
Non-targeting
#1
#2
#3
#4
#5
C
Non-targeting
#1
Inset
Mineralization (Alizarin Red)
D
Bone nodule area (%)
20
15
10
5
0.10
0.05
0.00
**
Non-targeting
#1
E
Differentiated MC3T3 osteoblasts (Day 21)
Relative fold expression (mRNA)
2.0
1.5
1.0
0.5
0.0
ALP
RUNX2
OCN
OSX
RANKL
MEPE
PHEX
GGPS1
Non-targeting
shRNA #1

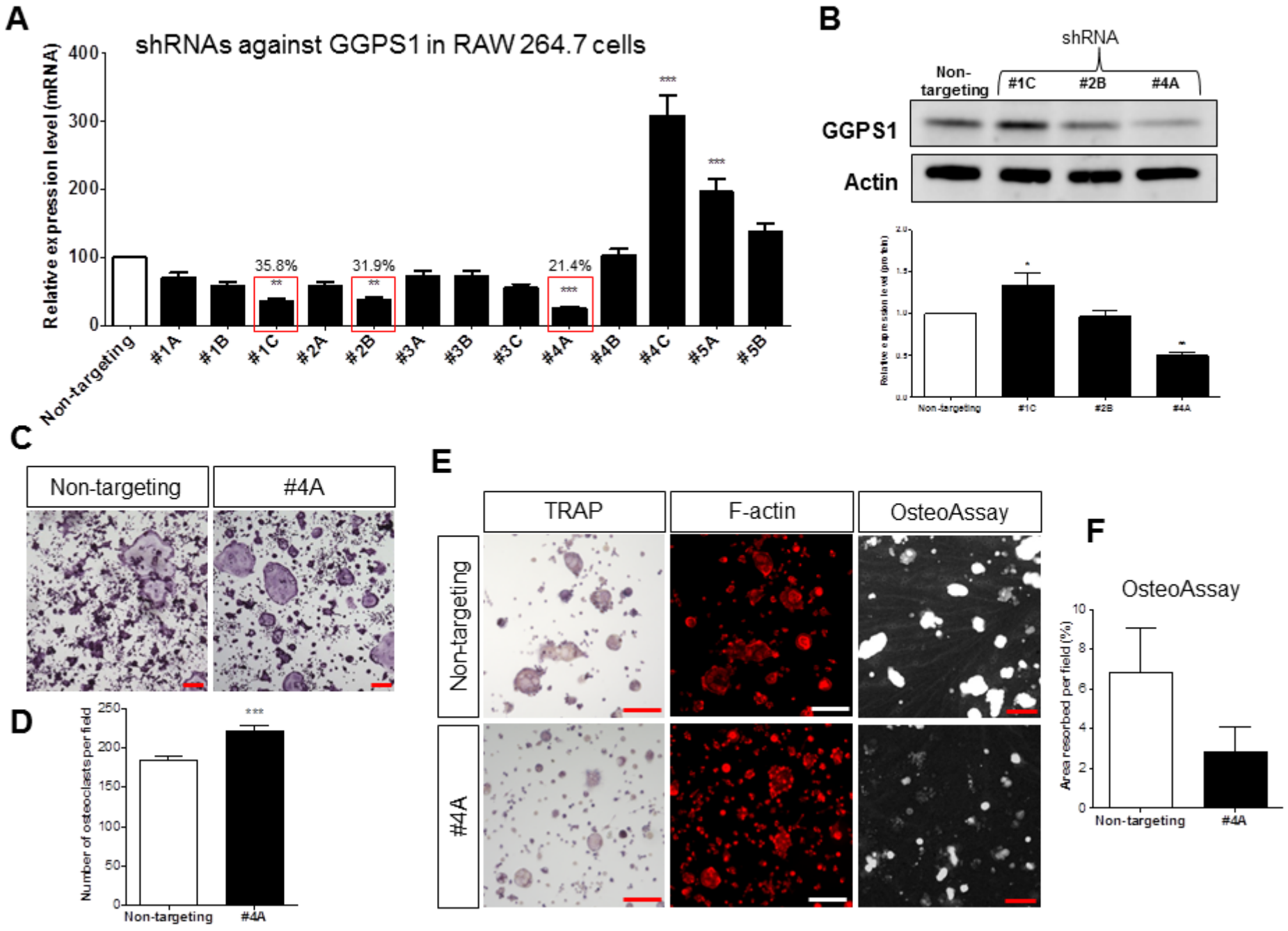
A
shRNAs against GGPS1 in RAW 264.7 cells
Relative expression level (mRNA)
400
300
200
100
0
35.8%
31.9%
21.4%
**
**
***
***
***
Non-targeting
#1A
#1B
#1C
#2A
#2B
#3A
#3B
#3C
#4A
#4B
#4C
#5A
#5B
B
shRNA
Non-targeting
#1C
#2B
#4A
GGPS1
Actin
Relative expression level (protein)
2.0
1.5
1.0
0.5
0.0
*
**
Non-targeting
#1C
#2B
#4A
C
Non-targeting
#4A
D
Number of osteoclasts per field
250
200
150
100
50
0
***
Non-targeting
#4A
E
TRAP
F-actin
OsteoAssay
Non-targeting
#4A
F
OsteoAssay
Area resorbed per field (%)
10
8
6
4
2
0
Non-targeting
#4A

FIGURE 4